Lee, J., Medina-Bailon, C., Berrada, S., Carrillo-Nunez, H., Sadi, T., Georgiev, V. P., Nedjalkov, M. and Asenov, A. (2019) A Multi-Scale Simulation Study of the Strained Si Nanowire FETs. In: 2018 IEEE 13th Nanotechnology Materials & Devices Conference (NMDC 2018), Portland, OR, USA, 14-17 Oct 2018, ISBN 9781538610169.

There may be differences between this version and the published version. You are advised to consult the publisher's version if you wish to cite from it.

http://eprints.gla.ac.uk/167522/

Deposited on: 23 August 2018

Enlighten – Research publications by members of the University of Glasgow
http://eprints.gla.ac.uk

A Multi-Scale Simulation Study of the Strained Si Nanowire FETs

Jaehyun Lee
School of Engineering
University of Glasgow
Glasgow, United Kingdom
Jaehyun.Lee@glasgow.ac.uk

Cristina Medina-Bailon
School of Engineering
University of Glasgow
Glasgow, United Kingdom
Cristina.MedinaBailon@glasgow.ac.uk

Salim Berrada
School of Engineering
University of Glasgow
Glasgow, United Kingdom
Salim.Berrada@glasgow.ac.uk

Hamilton Carrillo-Nunez
School of Engineering
University of Glasgow
Glasgow, United Kingdom
Hamilton.Carrillo-Nunez@glasgow.ac.uk

Toufik Sadi
Department of Neuroscience and Biomedical Engineering
Aalto Universityline
Aalto, Finland
toufik.sadi@aalto.fi

Vihar P. Georgiev
School of Engineering
University of Glasgow
Glasgow, United Kingdom
Vihar.Georgiev@glasgow.ac.uk

Mihail Nedjalkov
Institute for Microelectronics
TU-Vienna
Vienna, Austria
mixi@iue.tuwien.ac.at

Asen Asenov
School of Engineering
University of Glasgow
Glasgow, United Kingdom
Asen.Asenov@glasgow.ac.uk

***Abstract*— In this work, we study 2.1 nm-diameter uniaxial strained Si gate-all-around nanowire field-effect transistors, focusing on the electron mobility and the variability due to random discrete dopants (RDDs). Firstly, we extract the electron effective masses under various strains from Density Functional Theory (DFT) simulations. Secondly, we explore the impact of strain on the electron mobility in the Si nanowire using the Kubo-Greenwood formalism with a set of multi-subband phonon, surface roughness, and ionized impurity scattering mechanisms. Finally, we perform quantum transport simulations to investigate the effect of RDDs on the threshold voltage and the ON-state current variation.**

Keywords— DFT, Nanowire, Strain, Mobility

I. Introduction

Describing correctly quantum confinement is essential for predicting the electrical performance of Si nanowire (NW) field effect transistors (FETs). *Ab-inito* Hamiltonians based on tight-binding or Density Functional Theory (DFT) method can be directly used for charge transport simulations [1-2]. However, this approach is very inefficient in terms of computational cost. In this work, we propose a very efficient multi-scale simulation framework to study Si NW devices considering different uniaxial strain effects. In particular, it is important to perform statistical simulations with a large number of samples to investigate the impact of the random discrete dopants (RDDs), which are the dominant source of variability in the most cases [3].

As the size of a device shrinks to the nano-meter dimensions, electron mobility is degraded due to quantum confinement [4]. Strain engineering is one of the well-known methods of enhancing mobility. According to the International Roadmaps for Devices and Systems (IRDS), strain engineering is one of the key factors to improving device performance in sub-100nm technology [5]. The IRDS also reported that the electron mobility should be 100 $cm^2/V/s$ or more with 10 nm gate length. In 2012, Niquet *et al*. presented that the electron mobility of the 8-nm diameter Si NW can be varied from 200 to 1400 $cm^2/V/s$ with moderate strains [6]. However, the diameters of Si NWFETs to be used for sub-10 technology such as 5 nm technology node are expected to be smaller than 8 nm to reduce short channel effects. Thus, the Si NW device with 2.1 nm diameter is considered in this study in order to evaluate the device behaviour for the future nodes.

This work was supported by the European Union's Horizon 2020 research and innovation programme under grant agreement No 688101 SUPERAID7 and the U.K. EPSRC under Projects EP/P009972/1 and Project EP/S001131/1.

TABLE I. Transport Effective Masses of a Si NW with a 2.1 nm Diameter.

Valley	Transport Effective Masses (m_0)				
	-2 %	-1 %	0 %	1 %	2 %
X1	1.037	1.035	1.110	1.342	1.342
X3	0.352	0.355	0.357	0.360	0.361
X5	0.516	0.519	0.508	0.496	0.499

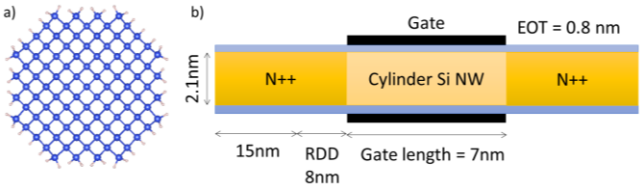

Fig. 1 a) The optimized atomic structures of the circular Si NW with the diameter of 2.1 nm. The transport direction is [100]. The blue and white spheres are Si and H atoms, respectively. b) The schematic diagram of the cylinder gate-all-around (GAA) Si Nanowire FETs. The gate length and equivalent oxide thickness (EOT) are 7 and 0.8 nm, respectively.

XXX-X-XXXX-XXXX-X/XX/$XX.00 ©20XX IEEE

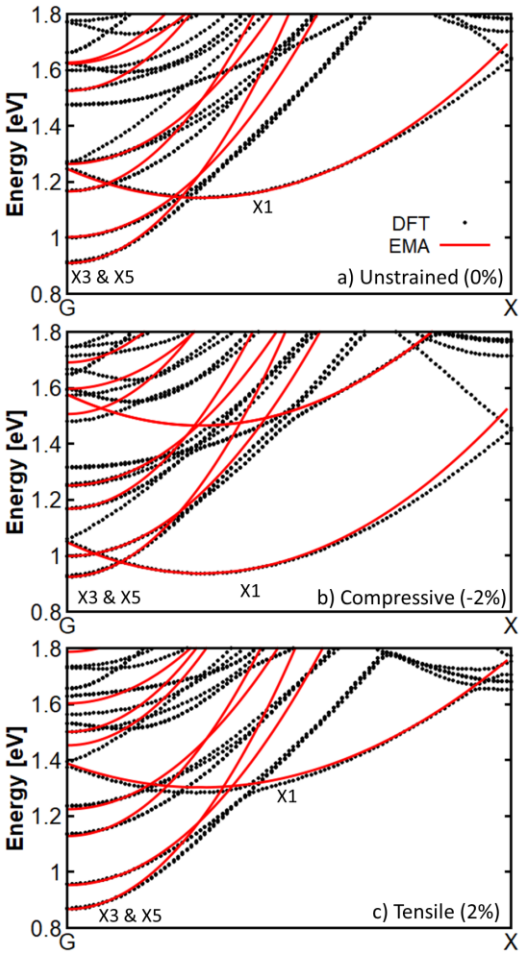

Fig. 2 DFT and EMA band structures of a 2.1 nm diameter intrinsic Si NW a) without strain and b) with 2% compressive and c) 2% tensile strains. The Fermi-level is set to 0.0 eV.

II. Simulation Approach

A. Extraction of the Effective Masses

In this work, we performe DFT simulations, implemented in the Atomistix Tool Kit from Synopsys QuantumWise [7], to calculate the band structure of Si NWs with and without uniaxial strain effects. The atomic structure of Si NWs, of which surface is passivated by hydrogen atoms (See Fig. 1 a)), is optimized until the maximum force on each atom becomes less than 10^{-2} eV/Å with the Generalized Gradient Approximation (GGA) as the exchange-correlation functional, as proposed by Perdew, Burke, and Ernzerhof [8]. The optimized lattice parameters of unstrained Si NWs is 5.515 Å, which is in agreement with the experimental value of 5.431 Å [9]. We examine ±1 and ±2 % uniaxial strains. Herein, '+' and '–' indicate tensile and compressive strain, respectively. In addition, the DFT(GGA)-1/2 method is used to accurately capture the Si bandgap and band structure. The calculated bandgaps of bulk Si and the unstrained Si NW with a 2.1 nm diameter are 1.175 and 1.820 eV, respectively.

Based on our DFT calculations, we extract the transport and confinement effective masses, which are used in device simulations. The former can directly be calculated using the definition of the effective mass from the band structure, $m^* = \hbar^2 \left(\partial^2 E / \partial k^2\right)^{-1}$, and the corresponding results are summarized in Table 1. The confinement effective masses are also calibrated to reproduce the energy levels of the first and the second conduction subbands.

B. Low-Field Mobility Calculation

The Kubo-Greenwood formalism based on the relaxation time approximation [10-12] is adopted to calculate the low-field electron mobility. The coupled 3D Poisson and 2D Schrödinger solver integrated in the TCAD simulator GARAND from Synopsys [13] is used to pre-calculate the required potential distributions and the corresponding Eigen functions. We consider all the important scattering mechanisms, including acoustic and optical phonon (Ph), surface roughness (SR), and ionized impurity (II) scatterings. The rate for each scattering process is calculated from Fermi's Golden rule accounting for the multi-subband quantization. For surface roughness scattering, we assume that the root mean square (RMS) roughness and correlation length are 0.48 and 1.3nm, respectively. The assumptions of the SR scattering model have been recently verified in [14]. A constant effective ionized impurity concentration $n_0 = 10^{18}$ cm^{-3} has been considered. Finally, the total mobility is calculated as a function of individual scattering-limited mobilities using the Matthiessen's rule [15].

C. Transport Simulation

The structure of cylindrical gate-all-around (GAA) Si NWFETs is shown in Fig. 1 b). The gate length, diameter of Si NW channel, and equivalent oxide thickness (EOT) are 7, 2.1, and 0.8 nm, respectively. The doping concentration of the source and drain is set to 10^{20} cm^{-3}. The source-drain voltage (V_{SD}) and the metal gate work function are 0.5 V and 4.55 eV, respectively. The source/drain are divided into two parts: the regions with uniformly distributed dopants and with RDDs. The former is essential for good convergence. The rejection scheme considering the Si atomic arrangement with the corresponding lattice parameters of unstrained and strained Si NW is applied to generate RDDs. For the statistical analysis, 94 (unstrained), 97 (-1%, 1%, and 2% strained), and 89 (-2% strained) well-converged devices are taken into account.

To describe electron transport in Si NWFETs, the effective mass Hamiltonian calibrated with DFT band structures is used in this study. The electron density and current are calculated by solving self-consistently Poisson and the coupled mode-space Non-Equilibrium Green's Function (NEGF) transport equations, which are implemented in Nano-Electronic Simulation Software (NESS) [16]. Hard wall boundary conditions are employed at the Si NW surface.

III. Results and Discussion

The effective mass approximation (EMA) successfully reproduces the DFT band structures of unstrained and strained 2.1 nm diameter Si NWs near the conduction band edge (CBE),

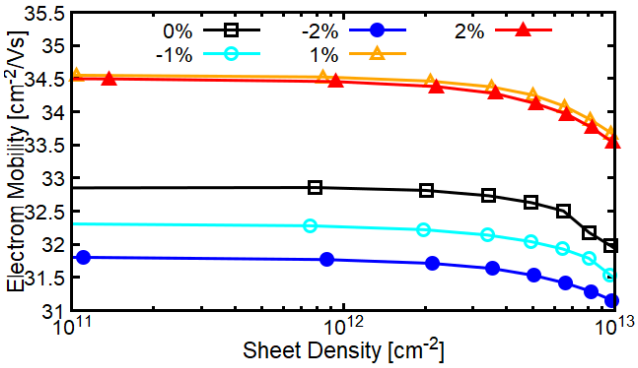

Fig. 3 The total low-field electron mobility as a function of the sheet density considering different uniaxial strain effects for a 2.1 nm diameter cylindrical Si NW.

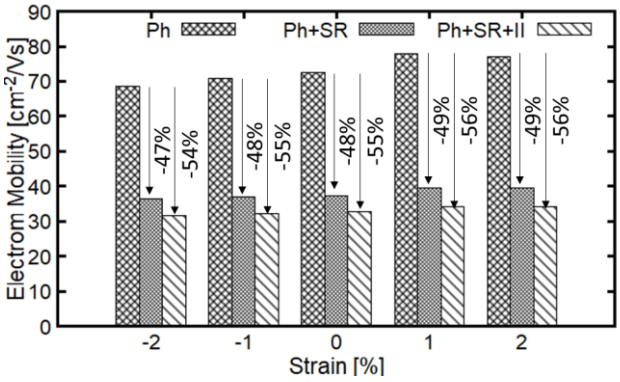

Fig. 4 The Ph-, Ph+SR-, and Ph+SR+II-limited low-field electron mobility with different uniaxial strains. The electron sheet density is $\mathbf{2 \times 10^{12}}$cm^{-2}

as can be seen in Fig. 2. As the large compressive strain is applied to the Si NW, the CBE of the X1 valley becomes smaller and eventually getting close to the CBE of X3 and X5 valleys under 2% uniaxial compressive strain. This behaviour is in good agreement with the results presented in [6].

In Fig. 3, the dependence of the low-field electron mobility on the electrical sheet density and the uniaxial strain effects is illustrated. The transport orientation is [100]. As the sheet density increases, the mobility decreases because of the SR scattering. It is highlighted that the overall mobility of the 2.1 nm diameter Si NW is much smaller than that of the 8 nm diameter Si NW, as presented in [6], and the criteria from the IDRS report [5], due to the larger transport effective masses. We found out that compressive strain degrades the mobility while the tensile strain enhances.

The low-field mobility from considering different scattering mechanisms is described in Fig. 4. This figure reveals that the phonon-limited mobility of the device under 2% compressive strain has the smallest value like the total mobility shown in Fig. 3. As expected, the effect of SR and II scatterings reduce mobilities, and the mobility reduction due to SR scattering dominates compared to II scattering. Remarkably, the impact of the scattering mechanisms does not depend on the applied strain.

Fig. 5 shows the drain current (I_D) - gate voltage (V_G) characteristics of 2.1 nm-diameter cylinder Si NWFETs under different uniaxial strains using the NEGF formalism in the

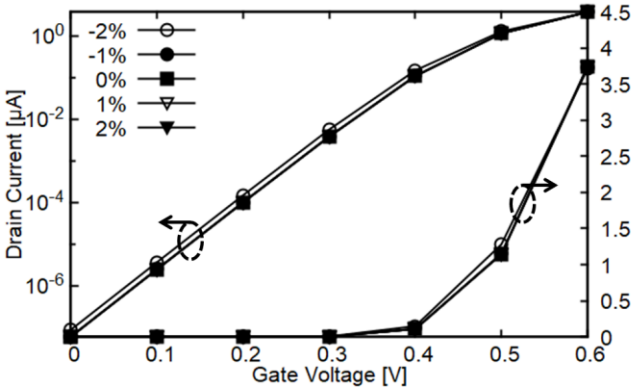

Fig. 5 Drain current - gate voltage characteristics with and without the uniaxial strain effects. An uniformly distributed doping profile is taken into account.

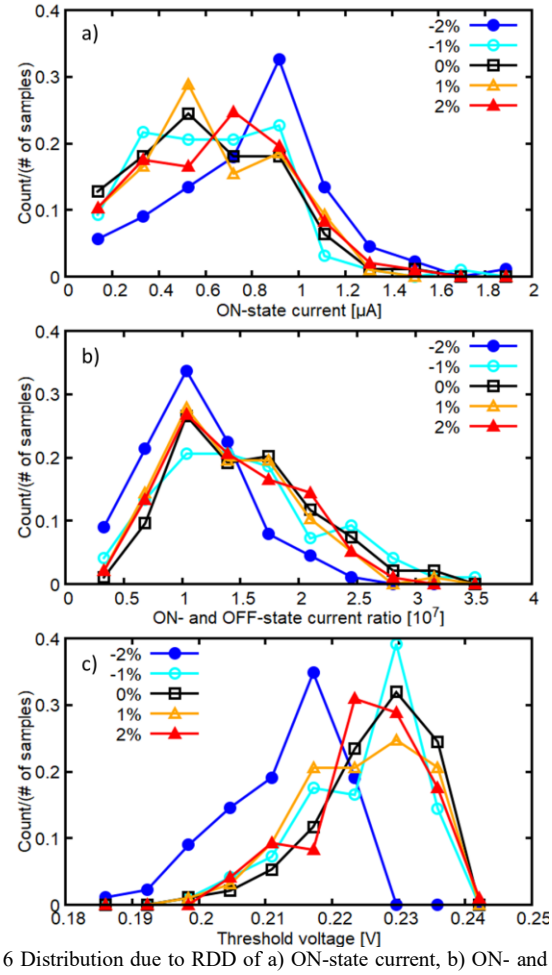

Fig. 6 Distribution due to RDD of a) ON-state current, b) ON- and OFF-state current ratio, and c) threshold voltage of devices with and without uniaxial strain effects.

ballistic limit. The source and drain of the devices are herein assumed to be uniformly doped. Similar to the calculated low-field mobility, the electrical performance of the device is hardly affected by strain effects. The ON-state current (I_{ON}) of the device under 2% uniaxial compressive strain, defined at $V_G = V_{SD} = 0.5$ V, is slightly larger (12%) compared to other devices although its mobility is smaller (See Figs 3 and 4). This

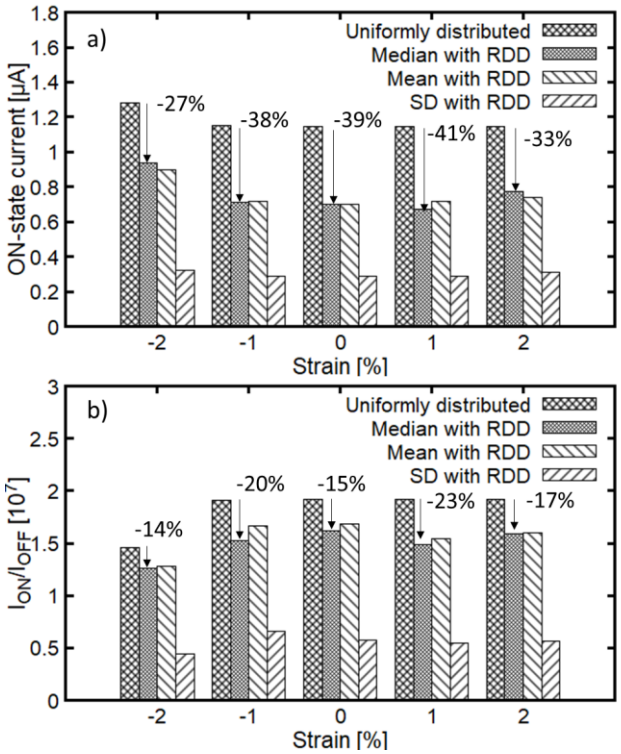

Fig. 7 Comparison of a) ON-state current and b) ON- and OFF-state current ratio with different uniaxial strain effects. SD indicates the standard deviation.

behaviour can be explained by the increase of carrier density due to the increase of X1 valley contribution (See Fig. 2).

Fig. 6 presents the distribution of I_{ON}, the ON- and OFF-state current ratio (I_{ON}/I_{OFF}), and the threshold voltage (V_{th}) induced by the RDDs. It is important to point out that only the devices under 2% compressive strain have significantly a different distribution in comparison to all other cases. Moreover, they have a smaller variation of I_{ON}/I_{OFF} than others. In terms of V_{th}, the peak of those devices is shifted by around -0.015 V in comparison to all other cases, but there is no significant difference in the shape of the distribution.

We investigate I_{ON} of devices under different uniaxial strains, as shown in Fig. 7 a). The median, mean values, and standard deviation (SD) of I_{ON} induced by RDDs are displayed together. As we explained above, the enhancement amount of I_{ON} thanks to a 2% compressive strain is just 12% compared to that of the unstrained device. However, we found out that it is improved by 34% after considering RDD effects. This is because the I_{ON} reduction rate due to RDDs is relatively small (27%). In this figure, it is also visible that the SD values of devices are comparable.

Finally, I_{ON}/I_{OFF} of devices under different uniaxial strains is studied in the same manner, as shown in Fig. 7 b). Due to the large OFF-state current of the device under 2% compressive strain (See Fig. 5), its I_{ON}/I_{OFF} is smaller compared to other cases. Moreover, from a smaller value of SD, we can see again that the devices under 2% compressive strain are less subject to variability problems due to RDDs.

IV. Conclusions

In this work, we have proposed a multi-scale simulation framework, combining atomistic and transport simulations, to study the uniaxial strain effects on Si nanowire (NW) field effect transistors. Our results show that no significant improvement in uniaxial strain is observed in such small diameter Si NWs in terms of both the low-field mobility and the ON-state current. This is a different result from the previous study presenting that the mobility of 8-nm diameter Si NWs is responsive to strain. Moreover, we have found out that 2% compressive strain can contribute to reducing ON-state current reduction and ON- and OFF-state current ratio variations induced by the random discrete dopants.

References

[1] M. Luisier and G. Klimeck, “Atomistic full-band simulations of silicon nanowire transistors: Effects of electron-phonon scattering”, Phys. Rev. B., vol. 80, pp. 155430, Oct. 2009.

[2] M. Shin, W. J. Jeong, and J. Lee, “Density Functional Theory Based Simulation of Silicon Nanowire Field Effect Transistors”, vol. 119, no. 15, pp. 154505, Apr. 2016.

[3] A. Martinez, M. Aldegunde, N. Seoane, A. R. Brown, J. R. Barker, and A. Asenov, “Quantum-Transport Study on the Impact of Channel Length and Cross Sections on Variability Induced by Random Discrete Dopants in Narrow Gate-All-Around Silicon Nanowire Transistors”, IEEE Trans. Electron Devices, vol. 58, no. 8, pp. 2209-2217, Aug. 2011.

[4] R. Rhyner and M. Luisier, “Phonon-limited low-field mobility in silicon: Quantum transport vs. linearized Boltzmann Transport Equation”, J. Appl. Phys., vol. 114, pp. 223708, Dec. 2013.

[5] International Roadmaps for Devices and Systems [online]. Available at https://irds.ieee.org/ [Accessed June 19, 2018].

[6] Y. M. Niquet, C. Delerue, and C. Krzeminski, “Effects of Strain on the Carrier Mobility in Silicon Nanowires”, Nano Lett., vol. 12, no. 7, pp. 3545-3550, June 2012.

[7] Atomistix ToolKit version 2017.2, Synopsys QuantumWise A/S. Available at http://www.quantumwise.com [Accessed June 19, 2018]

[8] J. P. Perdew, K. Burke, and M. Ernzerhof, ”Generalized Gradient Approximation Made Simple”, Phys. Rev. Lett., vol. 77, pp. 3865, Oct. 1996.

[9] H.W. King, CRC Handbook of Chemistry and Physics, vol. 83, p. 19. 2002,

[10] L. S. D. Esseni, P. Palestri, Nanoscale MOS Transistors: Semi-classical Transport And Applications. New York, USA: Cambridge University Press, 2011.

[11] D. Ferry and C. Jacoboni, Quantum transport in semiconductors. Berlin, Germany: Springer Science & Business Media, 1992.

[12] S. Jin, T.-W. Tang, and M. V. Fischetti, “Simulation of silicon nanowire transistors using Boltzmann transport equation under relaxation time approximation,” IEEE Trans. Electron Devices, vol. 55, no. 3, pp. 727–736, Feb. 2008.

[13] Garand User Guide, Available at https://solvnet.synopsys.com, Synopsys, inc., 2017.

[14] M. Nedjalkov, P. Ellinghaus, J. Weinbub, T. Sadi, A. Asenov, I. Dimov, and S. Selberherr, "Stochastic Analysis of Surface Roughness Models in Quantum Wires", Comput. Phys. Commun., vol. 228, pp. 30-37, July, 2018.

[15] D. Esseni, and F. Driussi. “A quantitative error analysis of the mobility extraction according to the Matthiessen rule in advanced MOS transistors”, IEEE Trans. Electron Devices, vol. 58, no. 8, p. 2415-2422, June 2011.

[16] S. Berrada, H. Carrillo-Nuñez, J. Lee, C. Medina-Bailon, T. Dutta, M. Duan, F. Adamu-Lema, V. Georgiev, and A. Asenov, “NESS: new flexible Nano-Electronic Simulation Software”, in Proc. SISPAD 2018.